Single-Molecule Observation of Anomalous Electrohydrodynamic Orientation of Microtubules

M. G. L. van den Heuvel,[1] R. Bondesan,[2] M. Cosentino Lagomarsino,[2] and C. Dekker[1]

[1]*Kavli Institute of Nanoscience, Delft University of Technology, Lorentzweg 1, 2628 CJ Delft, The Netherlands*
[2]*Dipartimento di Fisica, Università degli Studi di Milano and I.N.F.N., Via Celoria 16, 20133 Milano, Italy*

(Received 14 March 2008; published 9 September 2008)

We use fluorescence microscopy to measure the orientation and shape of microtubules—which serve as a model system for semiflexible rods—that are electrophoretically driven. Surprisingly, a bimodal orientation distribution is observed, with microtubules in either parallel or perpendicular orientations to the electric field. The occupancy of these states varies nonmonotonically with the microtubule length L and the electric field E. We also observe a surprising bending deformation of microtubules. Interestingly, all data collapse onto a universal scaling curve when the average alignment is plotted as a function of $B \propto EL^3$, which reflects the ratio between the driving force and a restoring elastic force. Our results have important implications for the interpretation of electrical birefringence experiments and, more generally, for a better understanding of the electrokinetics of rods.

DOI: 10.1103/PhysRevLett.101.118301 PACS numbers: 47.57.jd, 47.15.G−, 87.16.Ka

The electrophoresis of charged colloidal particles is central to diverse fields such as nanofluidics, colloid science, and biophysics. In particular, the orientation of rodlike semiflexible particles in an electric field is of interest. Fundamentally, it is relevant for an understanding of the electrophoretic behavior of important biological structures such as short DNA fragments and tobacco mosaic viruses, and of nonbiological colloidal rods such as micelles or polyelectrolytes. Practically, electro-optical measurement tools, such as electrical birefringence, are based on the electric-field-induced alignment of an ensemble of rodlike particles to measure their rotational dynamics and structural properties [1,2]. Interestingly however, in many cases anomalous birefringence signals are reported [1,3–5], indicating that a good microscopic understanding of the orientation mechanism in electric birefringence experiments is lacking.

The orientation of a homogeneously charged rodlike molecule in an electric field is expected to be governed by its polarizability, of which the largest contribution comes from the counterions [6]. The induced dipole moment that results from a displacement of the counterion cloud is largest along its long axis. Consequently, a rodlike particle is expected to align with its long axis parallel to the electric field. Moreover, for a homogeneously charged semiflexible rod in a homogeneous electric field, no deformation of the rod is expected.

Here, we present single-molecule measurements of the orientation and shape of charged semiflexible filaments in electric fields that show striking deviations from these simple predictions. Using fluorescence microscopy, we image the electrophoretic motion of microtubule filaments inside microfluidic channels [7]. Microtubules are stiff cylindrical biopolymers of 25 nm diameter and lengths L of several micrometers. Their large millimeter-size persistence length makes them an ideal model system for semiflexible rodlike particles. We observe an unexpected bimodal orientation distribution of microtubules, with orientations either in parallel or perpendicular alignment to the electric field. Interestingly, the average microtubule orientation exhibits a scaling behavior that indicates a balance between driving force and elastic deformation forces. The relevance of elasticity is further supported by the surprising observation that a subset of microtubules displays a pronounced U-shaped bending deformation. We suggest that these phenomena derive from an interplay between polarization and hydrodynamic interactions.

Microfluidic channels were fabricated as described previously [8]. Briefly, 500×1 μm slitlike channels were fabricated inside fused-silica substrates between reservoirs separated by 5 mm [Fig. 1(a)]. The inside of the channels is coated with casein to prevent surface interactions. Fluorescent microtubules [9] were added to the channel and

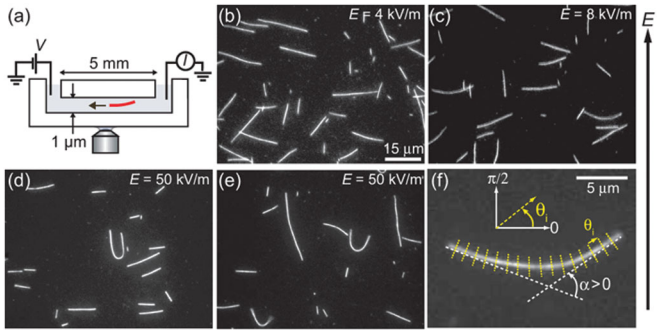

FIG. 1 (color). (a) Cross section of a microchannel, used to measure microtubule electrophoresis. With fluorescence microscopy, orientation and shape of microtubules are measured at different electric fields of (b) $E = 4$ kV/m, (c) 8 kV/m, and (d), (e) 50 kV/m. In all images the electric field points upwards (microtubules move downward). (f) For the analysis, each microtubule is divided in 1 μm long segments. Segment orientation θ_i and microtubule deformation angle α are defined in the picture.

observed through the glass. Electric fields were induced by applying a voltage via platinum electrodes in either reservoir.

Upon applying an electric field, negatively charged microtubules move toward the positive electrode. Their movement is a superposition of their electrophoretic movement and the electro-osmotic flow in the channel. The electro-osmotic flow velocity is opposite to, and smaller than, the electrophoretic velocity [8]. For electric fields $E = 2$–10 kV/m, the microtubule velocity was sufficiently low (less than ~ 0.13 mm/s) for taking fluorescence images using the minimum 20 ms integration time of our camera without significant motion blurring. For larger electric fields, measurements were obtained by applying an electric field during 1 s and taking a fluorescence image within 30 ms after switching off the electric field. This time is sufficiently short to limit significant rotational diffusion.

In Fig. 1(b), we show a fluorescence image taken during electrophoretic motion under $E = 4$ kV/m. The shortest microtubules in the image are mostly oriented parallel to the field. In contrast, the longest microtubules in this snapshot are predominantly oriented perpendicular to the field. Note that this is a surprising observation since polarization would drive long microtubules to a parallel orientation. At higher $E = 8$ kV/m [Fig. 1(c)] we find a similar preference for perpendicular orientation, apparently irrespective of microtubule length. Upon increasing the field further to $E = 50$ kV/m [Figs. 1(d) and 1(e)], we find that most short microtubules still have a perpendicular orientation, whereas longer microtubules now appear both in perpendicular and in parallel orientations.

In addition to the orientation of microtubules, we also observe an unexpected microtubule bending. Figure 1(c) shows two microtubules that are perpendicularly oriented and deformed in such a way that the microtubule ends point in the direction opposite to the direction of motion. At higher fields [Figs. 1(d) and 1(e)], this effect becomes so pronounced that microtubules are deformed into characteristic U shapes. Note that for a given E, microtubules of a given length can exist both in straight and parallel conformations as well as in U shapes, although the occurrence of U shapes is relatively low ($<10\%$).

We now quantify the orientation distribution of microtubules by measuring their orientation and length in a large number ($\sim$500–900) of fluorescence images. To account for bent microtubules, we divide each microtubule in 1 μm long segments, and measure for each segment its orientation θ_i and the length of the microtubule to which it belongs [Fig. 1(f)]. Segment orientations perpendicular to the field are denoted $\theta_i = 0$, whereas parallel orientations are denoted $\theta_i = \pi/2$. All angles are mapped onto the half-quadrant of $\theta_i \in [-\frac{1}{4}\pi, +\frac{3}{4}\pi]$.

In Fig. 2(a) we plot segment-orientation distributions for a selection of different electric fields and microtubule length in bins of 3 μm. Strikingly, we note that all distributions are clearly separated in two distinct states of parallel and perpendicular orientations, with a systematic change in the occupancy of these two states with L and E. For the lowest $E = 2$ kV/m (top row), we note that the shortest microtubules with $L \in [2, \ldots, 5]$ μm (denoted $[L] = 3.5$ μm, first column) have segment orientations that are randomly distributed, with a small peak around parallel orientations. For longer microtubules at this field strength, we note that initially the segments become oriented mostly parallel to the field. However, for the longest microtubules ($[L] \geq 15.5$ μm) the most probable segment orientation is perpendicular to the field, in accordance with the qualitative observations made in Fig. 1(b).

For higher $E = 6$ kV/m (second row) the same pattern is observed, with two differences: (i) for the shortest microtubule length, the parallel orientation peak is more pronounced, and (ii) the crossover between predominantly parallel and predominantly perpendicular orientations occurs at lower microtubule length (at $[L] = 12.5$ μm compared to $[L] = 15.5$ μm at $E = 2$ kV/m). At $E = 10$ kV/m, again we find that segment orientation is first predominantly parallel and subsequently perpendicular, and that the crossover again occurs at a lower length ($[L] = 9.5$ μm). A new phenomenon appears now as well: for the largest lengths ($[L] \geq 21.5$ μm) at this field strength, a second crossover is observed back towards parallel orientation. This second crossover, and the reduc-

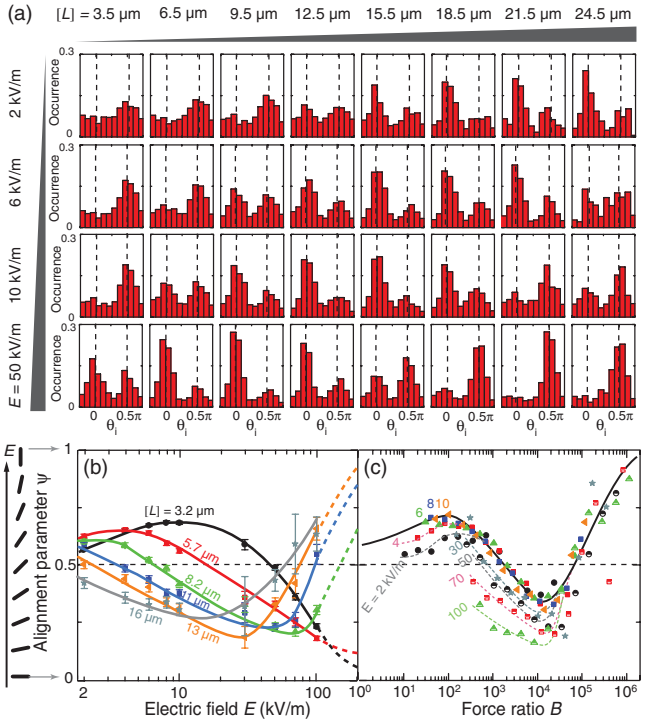

FIG. 2 (color). (a) Orientation distribution of microtubule segments separated on E (vertical axis) and into different length bins $[L]$ (horizontal axis, bin width 3 μm). (b) Alignment ψ as a function of E, for different microtubule length bins, bin width of 2.5 μm. Lines are guides to the eye. (c) Alignment ψ as function of force ratio B. Lines are guides to the eye.

ing trend in the length at which both crossovers occur, are further confirmed by the final set of distributions measured at an even higher $E = 50$ kV/m (bottom row).

The appearance of a bimodal orientation distribution of microtubule segments is a striking feature. The generic trend is that for short L and/or low E parallel orientations are favored, while for increasing either L or E a crossover to perpendicular orientation is observed, followed by a second crossover to parallel orientation. Note that this latter effect cannot be attributed only to U-shaped microtubules, which we checked by omitting these microtubules from the analysis. To parametrize these observations, we define a two-dimensional alignment parameter ψ that describes the average degree of segment alignment with the electric field:

$$\psi = \langle \sin^2(\theta_i) \rangle, \tag{1}$$

where $\langle \cdots \rangle$ averages over all microtubule segments analyzed. In this definition ψ changes from 0 for fully perpendicular orientation to 1 for complete parallel alignment, via $\psi = \frac{1}{2}$ for an isotropic distribution. This definition of ψ facilitates comparison of our data to electrical birefringence experiments, where the amount of birefringence is proportional to the average alignment of the molecules to the field [10].

In Fig. 2(b) we plot values of ψ as a function of E. As expected, we find that for the shortest length (black line, $[L] = 3.2$ μm) the alignment starts from an almost isotropic distribution for low E and progresses into parallel alignment. It then reaches a maximum of $\psi = 0.69$ for $E = 10$ kV/m, and decreases for larger E, progressing into perpendicular alignment with $\psi = 0.23$ at the largest E. Similar observations hold for $[L] = 5.7$ μm. For increasingly larger lengths, we only measure the decrease in ψ at low E, and we find that the crossing at $\psi = 0.5$ occurs at increasingly lower E. In addition, we find that for the longest lengths $[L] = 8.2$ to 15.7 μm a local minimum in ψ is reached and that the average alignment reverses into parallel orientation again for large E. The value of E at which the minimum occurs again decreases with increasing L.

Remarkably, when we plot the alignment parameter ψ as a function of a dimensionless force number B [11] instead of E, a near universal relationship $\psi(B)$ emerges over about 5 orders of magnitude in B [Fig. 2(c)]. The number $B \equiv \frac{\lambda L^3 E}{\kappa}$ reflects the ratio of the monopole driving force that acts on the microtubule ($\propto \lambda E L$, with λ the line-charge density of a microtubule [12]) and an elastic restoring force ($\propto \kappa / L^2$, with κ the microtubule stiffness [12]) that results from an elastic deformation of a microtubule [14]. For low B, ψ increases slowly toward a maximum at $B \approx 10^2$, indicating alignment parallel to E. Upon a further increase of B, ψ decreases, and beyond $B \approx 10^3$ the dominant orientation is perpendicular to E, with ψ reaching a minimum at $B \approx 10^4$. Finally, for even larger B, a second crossover is observed with a fast increase in ψ and a reversal to parallel orientation. Note that at low B a deviation from the universal curve is seen for small lengths at given $E = 2$ and 4 kV/m [black dotted line and red dotted line, respectively, in Fig. 2(c)]. Similarly, a deviation from universality is observed for the smallest lengths at large E of 30–100 kV/m.

The scaling with B implies that elastic deformations play an important role in the orientation mechanism. This is supported by the fact that we observe a characteristic U-shaped bending deformation of microtubules, in particular for microtubules that are oriented with their end-to-end vector perpendicular to E. We quantify the bending angle and show the results in Fig. 3. We define the bending angle α positive when both microtubule ends point in the direction opposite to the direction of motion [as in Fig. 1(f)], and negative when the ends point toward the direction of motion. Figure 3(a) shows binned values of α as a function of the average segment orientation of a microtubule $\langle \theta_i \rangle_{\mathrm{mt}}$, which equals the orientation of its end-to-end vector. For this plot we have mapped all angles onto $\langle \theta_i \rangle_{\mathrm{mt}} \in [0, \pi/2]$. Clearly, microtubules in perpendicular orientations ($\langle \theta_i \rangle_{\mathrm{mt}} = 0$) are much more bent than microtubules in parallel orientations ($\langle \theta_i \rangle_{\mathrm{mt}} = \pi/2$). Figure 3(b) shows that bending strongly increases with L and E. Note that within a single binned data point of α for given E and L, there is a considerable variance in α between individual micro-

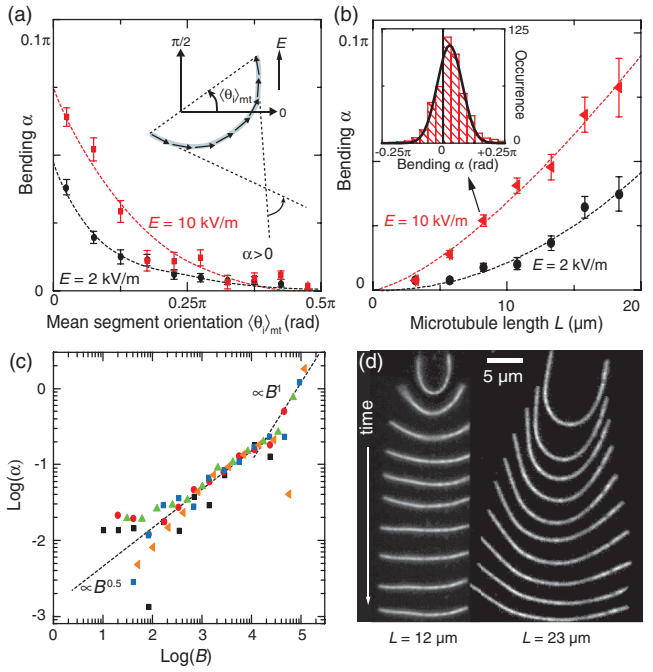

FIG. 3 (color). (a) Correlation between average microtubule orientation $\langle \theta_i \rangle_{\mathrm{mt}}$ and bending α. Lines are guides to the eye. (b) Microtubule bending α as a function of $[L]$, for 2 different E. Inset shows distribution of α for $E = 10$ kV/m and $[L] = 8.3$ μm. Lines are guides to the eye. (c) Bending as function of B for $E = 2$ (black square), 4 (red dots), 6 (green triangles), 8 (blue squares), and 10 kV/m (orange triangles). (d) Relaxation of 2 different microtubules after switching of the electric field. Snapshots are shown with 0.1 s time intervals.

tubules [inset of Fig. 3(b)]. Its distribution resembles a Gaussian, with the width of the distribution larger than its mean.

Interestingly, when α is plotted against B [Fig. 3(c)] we find a clear universal power law dependence with 2 different exponents. For $B < 10^2$ there is no universality, while for $B = 10^2$–10^4, $\alpha \propto B^{0.5}$, whereas for $B > 10^4$ it increases linearly with B. Note that the crossovers occur at similar values of B as the crossovers in ψ.

Finally, we confirm that the bending deformation of microtubules is a reversible effect which disappears after switching off the electric field. Figure 3(c) shows time-lapse images of two microtubules directly after switching off a field of $E = 40$ kV/m. The relaxation is a purely elastohydrodynamic effect and governed only by the microtubule stiffness and its length-dependent hydrodynamic drag [15], as is apparent from the more rapid relaxation of the short microtubule.

Our measurements have yielded the surprising insight that the orientations of microtubules in an electric field are distributed according to a bimodal distribution. Orientations are either parallel to the field, as would be expected from a polarization mechanism, or, remarkably, perpendicular to the field. The occupancy of either state is dependent on microtubule length and electric field. The second important observation is that the average alignment of microtubules, expressed in ψ, follows a near universal dependence on force ratio B with three clearly distinct regimes.

We suggest that our measurements can be interpreted as follows. The observations that in various regimes (i) orientation is essentially dependent on B and (ii) that it is associated with deformation suggest a role of hydrodynamic orientation, which has been explored numerically for the case of sedimentation [10,11]. Hydrodynamic interactions between different parts of a semiflexible filament were shown to lead to elastic U-shaped bending deformations, similar to what we observe. The reduction in symmetry then naturally leads to a coupling between translation and rotation [16], resulting in U shapes orienting perpendicular to the driving force. However, electrophoretic motion, as we have studied here, is fundamentally different due to the presence of the counterions, which make the hydrodynamic interactions much more short-range than in sedimentation [8]. We have performed simulations as described in Ref. [11], and replaced the hydrodynamic interaction tensor with an effective short-range electrophoretic interaction tensor [17]. Our simulations show that indeed a deformation-orientation effect occurs, which qualitatively explains the perpendicular orientations that we observe in our experiments.

We further speculate that the nonmonotonic $\psi(B)$ dependence results from a complex competition between polarization-driven parallel alignment and deformation-driven perpendicular alignment. We suggest that for $B < 10^2$, polarization-driven parallel alignment dominates and deformation-orientation effects are negligible, consistent with a nonuniversal dependence on B for both α and ψ [Figs. 2(c) and 3(c)]. For larger $B \geq 10^2$, however, deformation orientation becomes the stronger effect, resulting in perpendicular alignment. Finally, we propose that for $B > 10^4$ a third regime is entered where the induced dipole dominates because it scales faster than field-induced body force. Interestingly, the two crossovers in $\psi(B)$ and $\alpha(B)$ occur at similar values of B [Fig. 3(c)]. One could speculate that the second crossover is caused by an increased instability of U shapes.

In conclusion, our data provide the first systematic experimental investigation of the orientation of semiflexible filaments during electrophoresis at a single-molecule level. The results indicate an interesting interplay between electrohydrodynamics and polarization, for which further theoretical efforts are needed.

We acknowledge Roland Netz (Munich) for discussion and for providing us with a preprint of simulation results. This work was supported by FOM and NWO.

[1] C. T. Okonski and B. H. Zimm, Science **111**, 113 (1950).
[2] E. Fredericq and C. Houssier, *Electric Dichroism and Electric Birefringence* (Clarendon, Oxford, 1973).
[3] M. Hogan, N. Dattagupta, and D. M. Crothers, Proc. Natl. Acad. Sci. U.S.A. **75**, 195 (1978).
[4] H. Hoffmann, U. Kramer, and H. Thurn, J. Phys. Chem. **94**, 2027 (1990).
[5] U. Kramer and H. Hoffmann, Macromolecules **24**, 256 (1991).
[6] K. Lachenmayer and W. Oppermann, J. Chem. Phys. **116**, 392 (2002).
[7] T. Kim, M. T. Kao, E. F. Hasselbrink, and E. Meyhofer, Nano Lett. **7**, 211 (2007).
[8] M. G. L. van den Heuvel, M. P. de Graaff, S. G. Lemay, and C. Dekker, Proc. Natl. Acad. Sci. U.S.A. **104**, 7770 (2007).
[9] Microtubules were polymerized at 37 °C for 45 min from 5 mg/mL tubulin (1:3 stoichiometry of rhodamine labeled:unlabeled tubulin) and stabilized in 80 mM Pipes buffer containing 100 μM paclitaxel, supplemented with 0.13 M D-glucose, 0.13 mg/mL glucose oxidase, 0.06 mg/mL catalase, and 5% beta-mercapthoethanol to prevent photobleaching.
[10] X. Schlagberger and R. R. Netz, Europhys. Lett. **70**, 129 (2005).
[11] M. Cosentino Lagomarsino, I. Pagonabarraga, and C. P. Lowe, Phys. Rev. Lett. **94**, 148104 (2005).
[12] We calculate the line-charge density as $\lambda = 13 Q_{\mathrm{eff}}/8\,\mathrm{nm} = 10^{-8}\,\mathrm{C/m}$, assuming $Q_{\mathrm{eff}} = 23e^-$ per tubulin dimer of 8 nm length [8], and 13 protofilaments in parallel. For the stiffness we assume $\kappa = 2 \times 10^{-23}\,\mathrm{N m^2}$ [13].
[13] F. Gittes, B. Mickey, J. Nettleton, and J. Howard, J. Cell Biol. **120**, 923 (1993).
[14] Note that there is also a polarization induced dipole force, roughly proportional to $E^2 L$, which does not enter the definition of B.
[15] C. H. Wiggins, D. Riveline, A. Ott, and R. E. Goldstein, Biophys. J. **74**, 1043 (1998).
[16] H. Brenner, J. Fluid Mech. **12**, 35 (1962).
[17] D. Long and A. Ajdari, Eur. Phys. J. E **4**, 29 (2001).